Phosphine Complexes of Group 4 Metals. Synthesis, Structure, and Fluxional Behavior of Zirconium and Hafnium Butadiene Derivatives

Michael D. Fryzuk,* T. S. Haddad, and Steven J. Rettig†

Department of Chemistry, University of British Columbia, 2036 Main Mall, Vancouver, British Columbia, Canada V6T 1Y6

Received November 15, 1988

The reaction of magnesium butadiene $(Mg{\cdot}C_4H_6{\cdot}2THF)_n$ with the group 4 starting materials $MCl_3[N(SiMe_2CH_2PR_2)_2]$ (M = Zr, Hf; R = Me, Pr^i) generates good yields of butadiene complexes of the formula $M(\eta^4\text{-}C_4H_6)Cl[N(SiMe_2CH_2PR_2)_2]$. The remaining chloride of those derivatives having R = Me can be metathesized with alkyllithium reagents to generate hydrocarbyl complexes $M(\eta^4\text{-}C_4H_6)R'[N(SiMe_2CH_2PMe_2)_2]$ (M = Zr, Hf; R′ = Ph, CH_2CMe_3). The single-crystal, X-ray structures of $Zr(\eta^4\text{-}C_4H_6)Ph[N(SiMe_2CH_2PMe_2)_2]$ (monoclinic, space group $P2_1/c$, a = 16.483 (1) Å, b = 11.521 (1) Å, c = 14.168 (2) Å, β = 104.309 (7)°, Z = 4, $R = R_w$ = 0.041 for 2349 reflections with $I \geq 3\sigma(I)$) and $Hf(\eta^4\text{-}C_4H_6)Ph[N(SiMe_2CH_2PMe_2)_2]$ (monoclinic, space group $P2_1/c$, a = 16.323 (1) Å, b = 11.5063 (9) Å, c = 14.214 (2) Å, β = 104.450 (6)°, Z = 4, R = 0.033, and R_w = 0.034 for 3235 reflections with $I \geq 3\sigma(I)$) are reported. In solution, the spectroscopic data are consistent with the 1,3-butadiene moiety undergoing a diene rotation and not the envelope-flipping mechanism common to early metal diene complexes. It is proposed that the phosphine donors of the ancillary ligand help stabilize a M(II) contribution, thereby inducing substantial π-character in the bonding of the diene unit.

The considerable interest in 1,3-diene complexes of the group 4 metals is not surprising.[1] Out of this research has come a number of fundamental benchmark discoveries, such as the first mononuclear diene complex with the diene bound in the s-trans conformation[2] and a host of new reagents for organic[3] and organometallic[4] transformations. In addition, the bonding displayed by group 4 diene complexes, and early metal dienes in general,[5] has provided new insights on the effect of periodicity on the coordination modes of unsaturated hydrocarbon ligands.

The simplest acyclic conjugated diene is 1,3-butadiene, and it is a rather common ligand particularly for complexes of the later transition metals.[6] Coordination of 1,3-butadiene to these electron-rich metals takes the form of a π-bound, cis-planar set of carbon atoms all nearly equidistant from the metal as shown in A. In addition, the carbon–carbon bond lengths are usually very similar in the range 1.4–1.45 Å. This π,η^4-binding mode typifies 1,3-diene complexes of those metals to the right of the transition series. For the early transition metals and actinide elements,[7] a completely different mode of coordination is found which entails both σ- and π-components as shown in B. In this σ^2,π-geometry, the four bonding carbon atoms are not equidistant from the electron-deficient metal and the carbon–carbon bond lengths are quite dissimilar, alternating as long–short–long. An extreme view of this latter mode is as a metallocyclopentene moiety having a weak interaction of the distal π-system with the metal center.

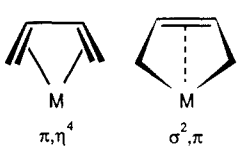

The dynamics of coordinated dienes also appear to depend on the position of the central metal in the transition series. For the later, electron-rich metals, the diene moiety normally undergoes rotation around the metal-to-centroid axis while for the early, electron-deficient metals, a process known as envelope or diene flipping is observed (Figure 1). However, this latter process has been induced in late metal complexes of the formula $(\eta^5\text{-}C_5H_5)Co$(1,3-diene) under photochemical conditions.[8] Speculation on diene rotation coupled with diene flipping for early metal complexes of molybdenum[9] and tungsten[10] has been reported.

As part of a general investigation of phosphine derivatives of the early and the lanthanoid metals, we examined the reaction of "magnesium butadiene", $(Mg{\cdot}C_4H_6{\cdot}2THF)_n$,

† Experimental Officer: UBC Crystal Structure Service.

(1) (a) Erker, G.; Kruger, C.; Muller, G. *Adv. Organometall. Chem.* **1985**, *24*, 1–39. (b) Yasuda, H.; Tatsumi, K.; Nakamura, A. *Acc. Chem. Res.* **1985**, *18*, 120–126. (c) Yasuda, H.; Nakamura, A. *Angew. Chem., Int. Ed. Engl.* **1987**, *26*, 723–742.

(2) (a) Erker, G.; Wicher, J.; Engel, K.; Rosenfeldt, F.; Dietrich, W.; Kruger, C. *J. Am. Chem. Soc.* **1980**, *102*, 6344–6346. (b) Kai, Y.; Kanehisa, N.; Miki, K.; Kasai, N.; Mashima, K.; Nagasuna, K.; Yasuda, H.; Nakamura, A. *J. Chem. Soc., Chem. Commun.* **1982**, 191–192.

(3) (a) Akita, M.; Yasuda, H.; Nakamura, A. *Chem. Lett.* **1983**, 217–218. (b) Mashima, K.; Yasuda, H.; Asami, K.; Nakamura, A. *Chem. Lett.* **1983**, 219–222. (c) Yasuda, H.; Nagasuna, K.; Asami, K.; Nakamura, A. *Chem. Lett.* **1983**, 955–958.

(4) (a) Yasuda, H.; Kajihara, Y.; Mashima, K.; Nagasuna, K.; Nakamura, A. *Chem. Lett.* **1981**, 671–674. (b) Yasuda, H.; Kajihara, Y.; Nagasuna, K.; Mashima, K.; Nakamura, A. *Chem. Lett.* **1981**, 719–722. (c) Erker, G.; Engel, K.; Dorf, U.; Atwood, J. L.; Hunter, W. E. *Angew. Chem., Int. Ed. Engl.* **1982**, *21*, 914. (d) Erker, G.; Engel, K.; Atwood, J. L.; Hunter, W. E. *Angew. Chem., Int. Ed. Engl.* **1983**, *22*, 494–495. (e) Erker, G.; Dorf, U. *Angew. Chem., Int. Ed. Engl.* **1983**, *22*, 777–778. (f) Erker, G.; Dorf, U.; Benn, R.; Reinhardt, R.-D.; Peterson, J. L. *J. Am. Chem. Soc.* **1984**, *106*, 7649–7650. (g) Erker, G.; Muhlenbernd, T.; Benn, R.; Rufinska, A.; Tainturier, G.; Gautheron, B. *Organometallics* **1986**, *5*, 1023–1028. (h) Erker, G.; Lecht, R.; Peterson, J. L.; Bonnemann, H. *Organometallics* **1987**, *6*, 1962–1967. (i) Erker, G.; Lecht, R.; Schlund, R.; Angermund, K.; Kruger, C. *Angew. Chem., Int. Ed. Engl.* **1987**, *26*, 666–668.

(5) (a) Tatsumi, K.; Yasuda, H.; Nakamura, A. *Isr. J. Chem.* **1983**, *23*, 145–150. (b) Yasuda, H.; Tatsumi, K.; Okamoto, T.; Mashima, K.; Lee, K.; Nakamura, A.; Kai, Y.; Kanehisa, N.; Kasai, N. *J. Am. Chem. Soc.* **1985**, *107*, 2410–2422.

(6) Davies, S. G. *Organotransition Metal Chemistry: Applications to Organic Synthesis*; Pergamon Press: *Oxford*, 1982; pp 53–62.

(7) (a) Smith, G. M.; Suzuki, H.; Sonnenberger, D. C.; Day, V. W.; Marks, T. J. *Organometallics* **1986**, *5*, 549–561. (b) Erker, G.; Muhlenbernd, T.; Benn, R.; Ruflinska, A. *Organometallics* **1986**, *5*, 402–404.

(8) Eaton, B.; King, J. A., Jr.; Vollhardt, K. P. C. *J. Am. Chem. Soc.* **1986**, *108*, 1359–1360.

(9) Faller, J. W.; Rosan, A. M. *J. Am. Chem. Soc.* **1977**, *99*, 4858–4859.

(10) Green, M. L. H.; Hare, P. M.; Bandy, J. A. *J. Organomet. Chem.* **1987**, *330*, 61–74.

0276-7333/89/2308-1723$01.50/0

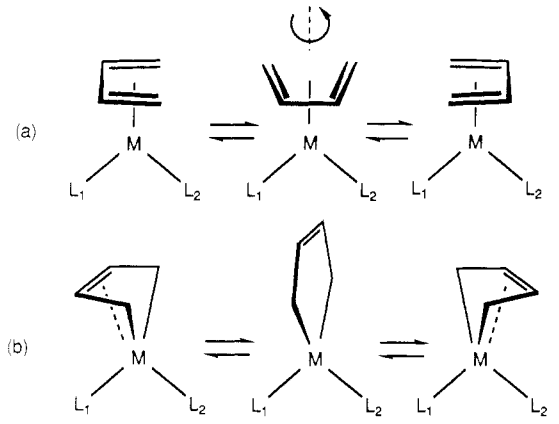

Figure 1. Fluxional processes for metal–diene complexes: (a) diene rotation about the metal-to-diene centroid axis; (b) envelope-flip mechanism. In both cases, the ligands L_1 and L_2 are equilibrated in the fast-exchange limit.

with the group 4 starting complexes $MCl_3[N(SiMe_2CH_2Pr_2)_2]$ (M = Zr(IV), Hf(IV); R = Me, Pr[i])[11] in an effort to access "lower" oxidation states of these metals. There is ample precedent that the phosphine donor stabilizes lower oxidation states; moreover, many of group 4 complexes in formal oxidation states of 2, 0, or lower have ancillary phosphine ligands.[12] Our particular ligand system incorporates the phosphine donors as part of a chelate array with an amido donor ($^-NR_2$, R = silyl) and thus allows coordination to metals in both high and low formal oxidation states.[13] In this paper, we report the synthesis, reactivity, and fluxional behavior of butadiene complexes of zirconium and hafnium[14] of the general formula $M(C_4H_6)Cl[N(SiMe_2CH_2PR_2)_2]$ (M = Zr, Hf; R = Me, Pr[i]). From solid-state structural data and solution-state variable-temperature NMR spectroscopic studies, it is concluded that the phosphine donors induce substantial π,η^4-character to these diene complexes resulting in the first unequivoval example[15] of diene rotation for group 4 metal diene derivatives.

Experimental Section

General Information. All manipulations were performed under prepurified nitrogen in a Vacuum Atmospheres HE-553-2 glovebox equipped with a MO-40-2H purification system or in standard Schlenk-type glassware on a dual vacuum/nitrogen line. $ZrCl_4$ and $HfCl_4$ (Aldrich) were sublimed prior to use. $LiCH_2CMe_3$,[16] LiPh,[17] $(Mg{\cdot}C_4H_6{\cdot}2THF)_n$,[18] and $MCl_3[N(SiMe_2CH_2PR_2)_2]$ (M = Hf or Zr; R = Me or Pr[i])[11] were prepared according to the literature procedures. 1,3-Butadiene (Matheson) was vacuum transferred from a −10 °C bath. Hexanes and THF were initially dried over CaH_2 followed by distillation from sodium–benzophenone ketyl. Diethyl ether and toluene were distilled from sodium–benzophenone ketyl. C_6D_6, C_7D_8, and spectral grade hexane were dried overnight with activated 4-Å molecular sieves, vacuum transferred to an appropriate container, "freeze–pump–thawed" three times, and stored in the glovebox. Carbon, hydrogen, and nitrogen analysis were performed by Mr. P. Borda of this department. ^1H NMR spectra (referenced to C_6D_5H at 7.15 ppm) were performed on one of the following instruments depending on the complexity of the particular spectrum: Bruker WP-80, Varian XL-300, or Bruker WH-400. ^{13}C NMR spectra (referenced to C_6D_6 at 128.0 ppm or $CD_3C_6D_5$ at 20.4 ppm) were run at 75.429 MHz, and $^{31}P\{^1H\}$ NMR spectra (referenced to external $P(OMe)_3$ at 141.0 ppm) were run at 121.421 MHz, both on a Varian XL-300. UV–vis spectra were obtained in hexane solutions on a Perkin-Elmer 552A spectrophotometer using a sealable quartz cell equipped with a Kontes Teflon needle valve. $\Delta G^\ddagger$ values were calculated from $^{31}P\{^1H\}$ NMR spectral data as reported earlier.[19]

$Zr(\eta^4\text{-}C_4H_6)Cl[N(SiMe_2CH_2PMe_2)_2]$ (2a). To a rapidly stirred solution of $ZrCl_3[N(SiMe_2CH_2PMe_2)_2]$ (1.487 g, 3.11 mmol) in THF (90 mL) was added a slurry of $(Mg{\cdot}C_4H_6{\cdot}2THF)_n$ (0.378 g, 1.70 mmol) in THF (10 mL) dropwise over a period of 5 min at room temperature. An instantaneous reaction occurred as the colorless Zr(IV) solution became deep orange. After the solution was stirred for 20 min, the solvent was removed under vacuum and the resulting oil was extracted with hexanes (50 mL). $MgCl_2$ was removed by filtration through Celite, and crystallization of the product was induced by cooling a saturated solution to −30 °C; yield 0.736 g (51%) of product. UV–vis (hexane): ϵ = 900 L mol^{-1} cm^{-1} at 350 nm. Anal. Calcd for $C_{14}H_{34}ClNP_2Si_2Zr$: C, 36.46; H, 7.43; N, 3.04. Found: C, 36.36; H, 7.50; N, 3.07.

$Hf(\eta^4\text{-}C_4H_6)Cl[N(SiMe_2CH_2PMe_2)_2]$ (2b). The identical procedure described above for the analogous zirconium compound was employed by using $HfCl_3[N(SiMe_2CH_2PMe_2)_2]$ (0.960 g, 1.70 mmol) and $(Mg{\cdot}C_4H_6{\cdot}2THF)_n$ (0.378 g, 1.70 mmol) yielding 0.746 g (80%). UV–vis (hexane): ϵ = 510 L mol^{-1} cm^{-1} at 420 nm and a shoulder at 350 nm. Anal. Calcd for $C_{14}H_{34}ClHfNP_2Si_2$: C, 30.66; H, 6.25; N, 2.55. Found: C, 30.41; H, 6.10; N, 2.46.

$Zr(\eta^4\text{-}C_4H_6)Cl[N(SiMe_2CH_2PPr^i_2)_2]$ (2c). The identical procedure described above for compound **2a** was employed by using $ZrCl_3[N(SiMe_2CH_2PPr^i_2)_2]$ (0.590 g, 1.000 mmol) and $(Mg{\cdot}C_4H_6{\cdot}2THF)_n$ (0.233 g, 1.047 mmol) yielding 0.448 g (78%) of product. Anal. Calcd for $C_{22}H_{50}ClNP_2Si_2Zr$: C, 46.08; H, 8.79; N, 2.44. Found: C, 45.94; H, 9.01; N, 2.61.

$Hf(\eta^4\text{-}C_4H_6)Cl[N(SiMe_2CH_2PPr^i_2)_2]$ (2d). The identical procedure described above for compound **2a** was employed by using $HfCl_3[N(SiMe_2CH_2PPr^i_2)_2]$ (2.163 g, 3.193 mmol) and $(Mg{\cdot}C_4H_6{\cdot}2THF)_n$ (0.752 g, 3.38 mmol) yielding 1.763 g (83%) of product. UV–vis (hexane): ϵ = 350 L mol^{-1} cm^{-1} at 450 nm and a shoulder at 360 nm. Anal. Calcd for $C_{22}H_{50}ClHfNP_2Si_2$: C, 39.99; H, 7.63; N, 2.12. Found: C, 40.00; H, 7.53; N, 2.08.

$Hf(\eta^4\text{-}C_4H_6)Ph[N(SiMe_2CH_2PMe_2)_2]$ (3b). Phenyllithium (0.025 g, 0.30 mmol) in ether (5 mL) was slowly added dropwise to a rapidly stirred ethereal solution (25 mL) of $Hf(\eta^4\text{-}C_4H_6)Cl[N(SiMe_2CH_2PMe_2)_2]$ (0.161 g, 0.294 mmol). After the solution was stirred for 15 min, the product was separated from the LiCl produced by removing the ether under vacuum, extracting with hexanes and filtering through a short column of Celite. Crystallization from minimum hexanes yielded 0.127 g of product (73%). Anal. Calcd for $C_{20}H_{39}HfNP_2Si_2$: C, 40.71; H, 6.66; N, 2.37. Found: C, 40.38; H, 6.60; N, 2.35.

(11) Fryzuk, M. D.; Carter, A.; Westerhaus, A. *Inorg. Chem.* **1985**, *24*, 642–648.

(12) (a) A recent monograph contains many such examples. Cardin, D. J.; Lappert, M. F.; Raston, C. L. *Chemistry of Organo-Zirconium and -Hafnium Compounds*; Wiley: New York, 1986. Some more recent examples are: (b) Stein, B. K.; Frerichs, S. R.; Ellis, J. E. *Organometallics* **1987**, *6*, 2017–2018. (c) Stein, B. K.; Frerichs, S. R.; Ellis, J. E. *J. Am. Chem. Soc.* **1987**, *109*, 5558–5560. (d) Blackburn, D. W.; Chi, K. M.; Frerichs, S. R.; Tinkham, M. L.; Ellis, J. E. *Angew. Chem., Int. Ed. Engl.* **1988**, *27*, 437–438. (e) Chi, K. M.; Frerichs, S. R.; Stein, B. K.; Blackburn, D. W.; Ellis, J. E. *J. Am. Chem. Soc.* **1988**, *110*, 163–171.

(13) (a) Fryzuk, M. D.; MacNeil, P. A. *J. Am. Chem. Soc.* **1981**, *103*, 3592–3593. (b) Fryzuk, M. D.; MacNeil, P. A. *J. Am. Chem. Soc.* **1984**, *106*, 6993–6999. (c) Fryzuk, M. D.; Rettig, S. J.; Westerhaus, A.; Williams, H. D. *Inorg. Chem.* **1985**, *24*, 4316–4325. (d) Fryzuk, M. D.; MacNeil, P. A.; Rettig, S. J. *J. Am. Chem. Soc.* **1985**, *107*, 6708–6710. (e) Fryzuk, M. D.; MacNeil, P. A.; Ball, R. G. *J. Am. Chem. Soc.* **1986**, *108*, 6414–6416. (f) Fryzuk, M. D.; MacNeil, P. A.; Rettig, S. J. *J. Am. Chem. Soc.* **1987**, *109*, 2803–2812.

(14) Some related work has been communicated in: Fryzuk, M. D.; Haddad, T. S.; Rettig, S. J. *Organometallics* **1988**, *7*, 1224–1226.

(15) Diene rotation has been discussed as a possibility in a series of papers relating to complexes of the formula $(\eta^5\text{-}C_5H_5)Zr(allyl)(diene)$, see: (a) Erker, G.; Berg, K.; Kruger, C.; Angermund, K.; Benn, R.; Schroth, G. *Angew. Chem., Int. Ed. Engl.* **1984**, *23*, 455–456. (b) Erker, G.; Berg, K.; Benn, R.; Schroth, G. *Angew. Chem., Int. Ed. Engl.* **1984**, *23*, 625–626. (c) Erker, G.; Berg, K.; Benn, R.; Schroth, G. *Chem. Ber.* **1985**, *118*, 1383–1397.

(16) Schrock, R. R.; Fellmann, J. D. *J. Am. Chem. Soc.* **1978**, *100*, 3359–3370.

(17) Schlosser, M.; Ladenberger, V. *J. Organomet. Chem.* **1967**, *8*, 193–197.

(18) Fujita, K.; Ohnuma, Y.; Yasuda, H.; Tani, H. *J. Organomet. Chem.* **1976**, *113*, 201–213.

(19) See ref 18 in Fryzuk, M. D.; MacNeil, P. A.; Rettig, S. J. *J. Am. Chem. Soc.* **1984**, *106*, 6993.

Table I. Crystallographic Data[a]

	3a	3b
formula	$C_{20}H_{39}NP_2Si_2Zr$	$C_{20}H_{39}HfNP_2Si_2$
fw	502.87	590.14
cryst system	monoclinic	monoclinic
space group	$P2_1/c$	$P2_1/c$
a, Å	16.483 (1)	16.323 (1)
b, Å	11.521 (1)	11.5063 (9)
c, Å	14.168 (2)	14.214 (2)
β, deg	104.309 (7)	104.450 (6)
V, Å^3	2607.0 (5)	2585.1 (4)
Z	4	4
D_{calcd}, g/cm^3	1.281	1.516
$F(000)$	1056	1184
radiatn	Cu	Mo
μ, cm^{-1}	56.2	42.2
cryst dimens, mm	0.30 × 0.35 × 0.57	0.18 × 0.27 × 0.30
transmissn factors	0.183–0.342	0.351–0.520
scan type	ω–2θ	ω–2θ
scan range, deg in ω	0.75 + 0.14 tan θ	0.65 + 0.35 tan θ
scan speed, deg/min	1.3–10.0	1.2–10.0
data collected	$\pm h,+k,+l$	$\pm h,+k,+l$
$2\theta_{max}$, deg	150	60
cryst decay	negligible	negligible
unique reflctns	5365	5924
reflctns with $I \geq 3\sigma(I)$	2349	3235
no. of variables	260	235
R	0.041	0.033
R_w	0.041	0.034
S	1.349	1.238
mean Δ/σ (final cycle)	0.020	0.004
max Δ/σ (final cycle)	0.43	0.04
residual density, e/Å^3	−0.8 to +0.8 (near Zr)	−0.7 to +1.3 (near Hf)

[a] Temperature 294 K; Enraf-Nonius CAD4-F diffractometer; Cu K_α radiation ($\lambda_{K\alpha_1}$ = 1.540 562, $\lambda_{K\alpha_2}$ = 1.544 390 Å); nickel filter; Mo K_α radiation ($\lambda_{K\alpha_1}$ = 0.709 30, $\lambda_{K\alpha_2}$ = 0.713 59 Å); graphite monochromator; takeoff angle 2.7°; aperature (2.0 + tan θ) × 4.0 mm at a distance of 173 mm from the crystal; scan range extended by 25% on both sides for background measurement; $\sigma^2(I) = C + 2B + [0.04(C - B)]^2$ (C = scan count, B = normalized background count); function minimized $\sum w(|F_o| - |F_c|)^2$ where $w = 1/\sigma^2F$); $R = \sum||F_o| - |F_c||/\sum|F_o|$; $R_w = (\sum w(|F_o| - |F_c|)^2/\sum w|F_o|^2)^{1/2}$; $S = (\sum w|F_o| - |F_c|)^2/(m - n))^{1/2}$. Values given for R, R_w, and S are based on those reflections with $I \geq 3\sigma(I)$.

Zr(η^4-C_4H_6)Ph[N(SiMe$_2$CH$_2$PMe$_2$)$_2$] (3a). The identical procedure described above for the analogous hafnium compound was employed by using Zr(η^4-C_4H_6)Cl[N(SiMe$_2$CH$_2$PMe$_2$)$_2$] (0.328 g, 0.711 mmol) and phenyllithium (0.060 g, 0.714 mmol) yielding 0.289 g (81%) of product. Anal. Calcd for $C_{20}H_{39}NP_2Si_2Zr$: C, 47.77; H, 7.82; N, 2.79. Found: C, 48.00; H, 7.79; N, 2.79.

Hf(η^4-C_4H_6)CH$_2$CMe$_3$[N(SiMe$_2$CH$_2$PMe$_2$)$_2$] (4b). To a hexane solution (20 mL) of Hf(η^4-C_4H_6)Cl[N(SiMe$_2$CH$_2$PMe$_2$)$_2$] (0.095 g, 0.17 mmol) was added neopentyllithium (0.013 g, 0.17 mmol) in hexanes (5 mL) dropwise with rapid stirring. After 15 min the cloudy solution was filtered through Celite to remove the LiCl produced, and the hexanes were removed under vacuum. Addition of a few drops of hexanes to the resulting oil induced instant crystallization. Enough hexanes were added to just redissolve these crystals, and cooling to −30 °C overnight yielded 0.077 g (76%) of pure product. Anal. Calcd for $C_{19}H_{45}HfNP_2Si_2$: C, 39.06; H, 7.76; N, 2.40. Found: C, 38.80; H, 7.86; N, 2.35.

Zr(η^4-C_4H_6)CH$_2$CMe$_3$[N(SiMe$_2$CH$_2$PMe$_2$)$_2$] (4a). The identical procedure described above for the analogous hafnium compound was employed by using Zr(η^4-C_4H_6)Cl[N(SiMe$_2$CH$_2$PMe$_2$)$_2$] (0.200 g, 0.434 mmol) and neopentyllithium (0.034 g, 0.44 mmol) yielding 0.125 g (58%) of product. Anal. Calcd for $C_{19}H_{45}NP_2Si_2Zr$: C, 45.93; H, 9.13; N, 2.82. Found: C, 45.60; H, 9.28; N, 3.10.

X-ray Crystallographic Analyses of Zr(η^4-C_4H_6)Ph[N(SiMe$_2$CH$_2$PMe$_2$)$_2$] (3a) and Hf(η^4-C_4H_6)Ph[N(SiMe$_2$CH$_2$PMe$_2$)$_2$] (3b). A summary of the refined cell parameters and relevant information regarding the data collection procedure is provided in Table I. The final unit-cell parameters were obtained by least squares on 2 (sin θ)/λ values for 25 reflections with 2θ = 50–80° for **3a** and 2θ = 30–40° for **3b**. The intensities of three standard reflections, measured each 4000 s of X-ray exposure time, showed only small (<4%) random fluctuations for both data collections. The data were processed and corrected for absorption (analytical method).[20]

The structure of the hafnium complex **3b** was solved by conventional heavy-atom methods. The Hf, P, and Si coordinates were determined from the Patterson function, and the remaining non-hydrogen atoms were positioned from a subsequent difference Fourier synthesis. The zirconium complex **3a** is isomorphous with **3b**; the refinement was initiatied by using the coordinates of the non-hydrogen atoms determined for the hafnium compound **3b**. All non-hydrogen atoms were refined with anisotropic thermal parameters. Hydrogen atoms were fixed in idealized positions (C(sp^2)–H = 0.97 Å, C(sp^3)–H = 0.98 Å, $U_H \propto U_{bonded\ atom}$). Out of interest, the hydrogen atoms on the C_4H_6 ligand of 3a were refined with isotropic thermal parameters. Neutral atom scattering factors and anomalous dispersion corrections (Hf, Zr, P, Si) were taken from the literature.[21] An isotropic type 1 extinction parameter[22–24] was refined for **3a**, the final value of g being 0.45 (3) × 10^4.

Final atomic coordinates and equivalent isotropic thermal parameters (U_{eq} = $^1/_3$ trace diagonalized U) are given in Table II. Bond lengths, bond angles, and intraannular torsion angles appear in Tables III–V, respectively. Calculated hydrogen atom parameters, anisotropic thermal parameters, bond lengths and angles involving refined hydrogen atoms, and structure factors (Tables S1–S6) are included as supplementary material.

Results and Discussion

Synthetic Considerations. The basic synthetic procedure employed was the reaction of the readily prepared[18] magnesium butadiene reagent (Mg·C_4H_6·2THF)$_n$ with the group 4 monoligand complexes $MCl_3[N(SiMe_2CH_2PR_2)_2]$ (1) as shown in eq 1. Colorless tetrahydrofuran (THF)

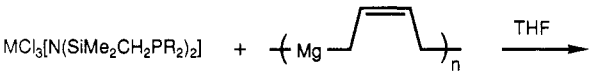

	M	R
1a	Zr	Me
1b	Hf	Me
1c	Zr	Pr^i
1d	Hf	Pr^i

(Mg·C_4H_6·2THF)$_n$

$M(C_4H_6)Cl[N(SiMe_2CH_2PR_2)_2]$ (1)

	M	R
2a	Zr	Me
2b	Hf	Me
2c	Zr	Pr^i
2d	Hf	Pr^i

solutions of the starting materials react instantly with the butadiene reagent to generate orange hafnium and red zirconium complexes of the formula M(η^4-C_4H_6)Cl[N(SiMe$_2$CH$_2$PR$_2$)$_2$] (**2**) as crystalline solids in good isolated yields. These hydrocarbon-soluble derivatives are thermally stable in the solid-state and solution at room temperature under nitrogen for months but are immediately decomposed by exposure to air or moisture in any phase.

The formation of Hf(η^4-C_4H_6)Cl[N(SiMe$_2$CH$_2$PMe$_2$)$_2$] (**2b**) was monitored by low-temperature (−78 °C) $^{31}P\{^1H\}$

(20) The computer programs used include locally written programs for data processing and locally modified versions of the following: ORFLS, full-matrix least-squares, and ORFFE, function and errors, by W. R. Busing, K. O. Martin, and H. A. Levy; FORDAP, Patterson and Fourier syntheses, by A. Zalkin; ORTEP II, illustrations, by C. K. Johnson; AGNOST, absorption corrections, by J. A. Ibers; MULTAN 80, multisolution program by P. Main, S. J. Fiske, S. E. Hull, L. Lessinger, G. Germain, J. P. Declercq, and M. M. Woolfson.

(21) *International Tables for X-ray Crystallography*; Kynoch Press: Birmingham, England, 1974; Vol. IV, pp 99–102, 149 (Present distributor D. Reidel, Dorfrecht).

(22) Becker, P. J.; Coppens, P. *Acta Crystallogr., Sect. A* **1974**, *A30*, 129–147, 148–153; **1975**, *A31*, 417–425.

(23) Coppens, P.; Hamilton, W. C. *Acta Crystallogr., Sect. A* **1970**, *A26*, 71–83.

(24) Thornley, F. R.; Nelmes, R. J. *Acta Crystallogr., Sect. A* **1974**, *A30*, 748–757.

Table II. Final Positional (Fractional ×10⁴; Hf, Zr, P, and Si ×10⁵) and Isotropic Thermal Parameters ($U \times 10^3$ Å²) with Estimated Standard Deviations in Parentheses

atom	x	y	z	U_{eq}/U_{iso}
	$Zr(C_4H_6)Ph[N(SiMe_2CH_2PMe_2)_2]$ (**3a**)			
Zr	29765 (4)	48941 (5)	38706 (5)	46
P(1)	16310 (12)	47525 (16)	46912 (16)	50
P(2)	36717 (13)	44320 (19)	23511 (19)	62
Si(1)	11300 (13)	62721 (17)	29410 (19)	51
Si(2)	17722 (13)	47814 (18)	15547 (17)	51
N	1861 (3)	5299 (4)	2714 (4)	40
C(1)	3770 (8)	5011 (14)	5543 (10)	91
C(2)	3365 (7)	6086 (11)	5373 (10)	84
C(3)	3361 (7)	3801 (10)	4613 (11)	84
C(4)	3834 (7)	6532 (10)	3911 (11)	82
C(5)	3204 (5)	2910 (6)	4014 (6)	54
C(6)	2563 (5)	2109 (8)	3584 (7)	67
C(7)	2681 (7)	918 (8)	3577 (8)	86
C(8)	3459 (9)	476 (9)	3977 (8)	92
C(9)	4099 (7)	1202 (9)	4419 (8)	91
C(10)	3972 (5)	2381 (7)	4433 (7)	71
C(11)	1097 (4)	6098 (6)	4240 (6)	55
C(12)	2740 (5)	3897 (6)	1516 (6)	55
C(13)	1664 (6)	4625 (8)	5987 (7)	79
C(14)	843 (5)	3668 (6)	4168 (7)	65
C(15)	4475 (5)	3324 (8)	2352 (7)	88
C(16)	4006 (6)	5641 (9)	1714 (8)	98
C(17)	27 (5)	6005 (7)	2206 (7)	68
C(18)	1387 (6)	7808 (6)	2717 (7)	78
C(19)	1637 (6)	5964 (8)	635 (7)	84
C(20)	868 (5)	3764 (7)	1145 (7)	75
H(1a)	369 (5)	436 (8)	607 (6)	106 (37)
H(1b)	418 (7)	507 (11)	550 (9)	65 (54)
H(2)	302 (4)	635 (6)	572 (6)	55 (27)
H(3)	296 (5)	740 (7)	446 (6)	72 (29)
H(4a)	364 (5)	709 (7)	326 (6)	95 (37)
H(4b)	436 (5)	629 (7)	428 (6)	74 (29)
	$Hf(C_4H_6)Ph[N(SiMe_2CH_2PMe_2)_2]$ (**3b**)			
Hf	29901 (2)	49109 (2)	38603 (2)	34
P(1)	16595 (12)	47581 (14)	46865 (13)	42
P(2)	36844 (13)	44078 (17)	23666 (16)	49
Si(1)	11239 (12)	62705 (15)	29422 (16)	41
Si(2)	17752 (12)	47887 (16)	15605 (14)	42
N	1879 (3)	5316 (4)	2725 (4)	33
C(1)	3819 (5)	5116 (7)	5486 (6)	70
C(2)	3352 (5)	6164 (7)	5311 (6)	62
C(3)	3334 (5)	6853 (7)	4548 (8)	63
C(4)	3817 (5)	6569 (6)	3857 (7)	67
C(5)	3169 (4)	2939 (6)	3995 (5)	38
C(6)	2560 (5)	2118 (6)	3548 (5)	47
C(7)	2691 (6)	936 (7)	3575 (7)	67
C(8)	3478 (8)	506 (7)	4027 (7)	78
C(9)	4109 (6)	1238 (8)	4459 (7)	71
C(10)	3957 (5)	2424 (7)	4451 (6)	56
C(11)	1102 (5)	6083 (6)	4256 (6)	48
C(12)	2739 (5)	3912 (6)	1519 (5)	46
C(13)	1710 (6)	4624 (7)	5989 (6)	68
C(14)	875 (5)	3649 (6)	4200 (6)	60
C(15)	4476 (6)	3293 (8)	2381 (7)	80
C(16)	4071 (6)	5589 (8)	1737 (7)	83
C(17)	12 (4)	5994 (7)	2212 (6)	61
C(18)	1368 (5)	7810 (6)	2707 (7)	68
C(19)	1646 (6)	5987 (8)	639 (7)	77
C(20)	855 (5)	3780 (7)	1141 (6)	66

NMR spectroscopy to check if resonances due to any intermediate species might be observable. Even at these low temperatures, the resonances characteristic of the product were observed to grow in with time, but no intermediates could be detected; only starting material, **1b**, and product were observed as the reaction proceeded. By comparison, the corresponding reaction of zirconocene dichloride, $(\eta^5\text{-}C_5H_5)_2ZrCl_2$, with $(Mg{\cdot}C_4H_6{\cdot}2THF)_n$ proceeds through the formation of the isolable s-trans isomer[25] which subsequently thermally isomerizes to the more stable s-cis form. In our case, this is possible but we cannot substantiate such a mechanism.

(25) Dorf, U.; Engel, K.; Erker, G. *Organometallics* **1983**, *2*, 462–463.

Table III. Bond Lengths (Å) with Estimated Standard Deviations in Parentheses

	$Zr(C_4H_6)Ph[N(SiMe_2CH_2PMe_2)_2]$ (**3a**)		
Zr-P(1)	2.752 (2)	Si(1)-C(11)	1.866 (9)
Zr-P(2)	2.730 (2)	Si(1)-C(17)	1.884 (8)
Zr-N	2.190 (6)	Si(1)-C(18)	1.865 (8)
Zr-C(1)	2.410 (12)	Si(2)-N	1.719 (6)
Zr-C(2)	2.481 (11)	Si(2)-C(12)	1.905 (7)
Zr-C(3)	2.450 (9)	Si(2)-C(19)	1.860 (9)
Zr-C(4)	2.350 (10)	Si(2)-C(20)	1.872 (9)
Zr-C(5)	2.317 (7)	C(1)-C(2)	1.40 (2)
Zr-B	2.056 (7)	C(2)-C(3)	1.354 (15)
P(1)-C(11)	1.818 (7)	C(3)-C(4)	1.442 (15)
P(1)-C(13)	1.829 (9)	C(5)-C(6)	1.422 (11)
P(1)-C(14)	1.823 (8)	C(5)-C(10)	1.398 (10)
P(2)-C(12)	1.800 (8)	C(6)-C(7)	1.386 (12)
P(2)-C(15)	1.839 (8)	C(7)-C(8)	1.365 (14)
P(2)-C(16)	1.818 (10)	C(8)-C(9)	1.370 (14)
Si(1)-N	1.733 (5)	C(9)-C(10)	1.376 (11)
	$Hf(C_4H_6)Ph[N(SiMe_2CH_2PMe_2)_2]$ (**3b**)		
Hf-P(1)	2.720 (2)	Si(1)-C(11)	1.889 (8)
Hf-P(2)	2.707 (2)	Si(1)-C(17)	1.880 (8)
Hf-N	2.157 (5)	Si(1)-C(18)	1.865 (7)
Hf-C(1)	2.380 (8)	Si(2)-N	1.731 (6)
Hf-C(2)	2.464 (7)	Si(2)-C(12)	1.883 (7)
Hf-C(3)	2.447 (7)	Si(2)-C(19)	1.877 (8)
Hf-C(4)	2.338 (7)	Si(2)-C(20)	1.874 (8)
Hf-C(5)	2.290 (6)	C(1)-C(2)	1.415 (10)
Hf-B	2.047 (4)	C(2)-C(3)	1.337 (12)
P(1)-C(11)	1.803 (7)	C(3)-C(4)	1.442 (12)
P(1)-C(13)	1.839 (8)	C(5)-C(6)	1.403 (9)
P(1)-C(14)	1.818 (8)	C(5)-C(10)	1.418 (9)
P(2)-C(12)	1.797 (7)	C(6)-C(7)	1.376 (10)
P(2)-C(15)	1.817 (8)	C(7)-C(8)	1.376 (13)
P(2)-C(16)	1.825 (9)	C(8)-C(9)	1.354 (13)
Si(1)-N	1.735 (5)	C(9)-C(10)	1.387 (10)

For the butadiene compounds **3a** and **4a**, having methyl groups on the phosphorus donors, the remaining chloride is labile and can be metathesized with phenyllithium or neopentyllithium to generate the corresponding hydrocarbyl derivatives (eq 2); the corresponding reactions of the complexes having isopropyl substituents on phosphorus (**2c** and **2d**) were not examined. The reaction of all of these butadiene derivatives **2a–d** with allylmagnesium chloride has been investigated, but as these complexes undergo an intramolecular carbon–carbon bond coupling, they will be discussed elsewhere.[14]

$$M(C_4H_6)Cl[N(SiMe_2CH_2PMe_2)_2] + R'Li \xrightarrow{THF} M(C_4H_6)R'[N(SiMe_2CH_2PMe_2)_2] \quad (2)$$

M	
2a	Zr
2b	Hf

	M	R'
3a	Zr	Ph
3b	Hf	Ph

	M	R'
4a	Zr	CH_2CMe_3
4b	Hf	CH_2CMe_3

Solid-State X-ray Structures of $Zr(\eta^4\text{-}C_4H_6)Ph[N(SiMe_2CH_2PMe_2)_2]$ and $Hf(\eta^4\text{-}C_4H_6)Ph[N(SiMe_2CH_2PMe_2)_2]$. The molecular structures and atom-labeling schemes of the zirconium phenyl complex **3a** and the corresponding hafnium derivative **3b** are shown in Figure 2. Because these compounds are virtually isostructural, the discussion will center on the zirconium

Table IV. Bond Angles (deg) with Estimated Standard Deviations in Parentheses

$Zr(C_4H_6)Ph[N(SiMe_2CH_2PMe_2)_2]$ (**3a**)			
P(1)-Zr-P(2)	149.43 (7)	C(11)-Si(1)-C(17)	105.6 (4)
P(1)-Zr-N	73.36 (15)	C(11)-Si(1)-C(18)	109.5 (4)
P(1)-Zr-C(5)	91.9 (2)	C(17)-Si(1)-C(18)	106.8 (4)
P(1)-Zr-B	93.4 (2)	N-Si(2)-C(12)	109.8 (3)
P(2)-Zr-N	83.66 (15)	N-Si(2)-C(19)	112.5 (4)
P(2)-Zr-C(5)	77.7 (2)	N-Si(2)-C(20)	112.7 (3)
P(2)-Zr-B	116.3 (2)	C(12)-Si(2)-C(19)	109.1 (4)
N-Zr-C(5)	111.3 (2)	C(12)-Si(2)-C(20)	105.3 (4)
N-Zr-B	122.8 (2)	C(19)-Si(2)-C(20)	107.0 (5)
C(5)-Zr-B	124.8 (3)	Zr-N-Si(1)	119.5 (3)
Zr-P(1)-C(11)	99.9 (2)	Zr-N-Si(2)	119.9 (3)
Zr-P(1)-C(13)	127.0 (3)	Si(1)-N-Si(2)	120.2 (3)
Zr-P(1)-C(14)	115.9 (3)	C(1)-C(2)-C(3)	125.7 (13)
C(11)-P(1)-C(13)	108.2 (4)	C(2)-C(3)-C(4)	121.4 (12)
C(11)-P(1)-C(14)	102.0 (4)	Zr-C(5)-C(6)	121.1 (6)
C(13)-P(1)-C(14)	101.2 (4)	Zr-C(5)-C(10)	125.3 (6)
Zr-P(2)-C(12)	97.4 (2)	C(6)-C(5)-C(10)	113.4 (7)
Zr-P(2)-C(15)	125.2 (3)	C(5)-C(6)-C(7)	123.7 (9)
Zr-P(2)-C(16)	118.7 (4)	C(6)-C(7)-C(8)	119.0 (10)
C(12)-P(2)-C(15)	105.1 (4)	C(7)-C(8)-C(9)	120.0 (9)
C(12)-P(2)-C(16)	104.5 (4)	C(8)-C(9)-C(10)	120.4 (9)
C(15)-P(2)-C(16)	103.1 (5)	C(5)-C(10)-C(9)	123.4 (9)
N-Si(1)-C(11)	107.7 (3)	P(1)-C(11)-Si(1)	108.0 (4)
N-Si(1)-C(17)	114.3 (3)	P(2)-C(12)-Si(2)	112.5 (4)
N-Si(1)-C(18)	112.6 (3)		
$Hf(C_4H_6)Ph[N(SiMe_2CH_2PMe_2)_2]$ (**3b**)			
P(1)-Hf-P(2)	149.36 (6)	C(11)-Si(1)-C(17)	105.8 (4)
P(1)-Hf-N	74.00 (14)	C(11)-Si(1)-C(18)	110.1 (4)
P(1)-Hf-C(5)	89.9 (2)	C(17)-Si(1)-C(18)	106.4 (4)
P(1)-Hf-B	93.47 (13)	N-Si(2)-C(12)	109.6 (3)
P(2)-Hf-N	84.12 (14)	N-Si(2)-C(19)	112.1 (3)
P(2)-Hf-C(5)	77.5 (2)	N-Si(2)-C(20)	113.6 (3)
P(2)-Hf-B	116.30 (13)	C(12)-Si(2)-C(19)	108.7 (4)
N-Hf-C(5)	110.1 (2)	C(12)-Si(2)-C(20)	105.6 (3)
N-Hf-B	120.4 (2)	C(19)-Si(2)-C(90)	106.9 (4)
C(5)-Hf-B	128.3 (2)	Hf-N-Si(1)	120.4 (3)
Hf-P(1)-C(11)	100.9 (2)	Hf-N-Si(2)	120.2 (3)
Hf-P(1)-C(13)	126.9 (3)	Si(1)-N-Si(2)	119.2 (3)
Hf-P(1)-C(14)	116.3 (3)	C(1)-C(2)-C(3)	123.4 (8)
C(11)-P(1)-C(13)	107.7 (4)	C(2)-C(3)-C(4)	120.8 (8)
C(11)-P(1)-C(14)	102.5 (4)	Hf-C(5)-C(6)	124.6 (5)
C(13)-P(1)-C(14)	100.0 (4)	Hf-C(5)-C(10)	122.3 (5)
Hf-P(2)-C(12)	97.9 (2)	C(6)-C(5)-C(10)	112.7 (6)
Hf-P(2)-C(15)	125.3 (3)	C(5)-C(6)-C(7)	124.4 (7)
Hf-P(2)-C(16)	119.3 (3)	C(6)-C(7)-C(8)	119.2 (8)
C(12)-P(2)-C(15)	105.8 (4)	C(7)-C(8)-C(9)	120.3 (7)
C(12)-P(2)-C(16)	104.6 (4)	C(8)-C(9)-C(10)	119.6 (8)
C(15)-P(2)-C(16)	101.5 (4)	C(5)-C(10)-C(9)	123.7 (8)
N-Si(1)-C(11)	107.1 (3)	P(1)-C(11)-Si(1)	107.4 (4)
N-Si(1)-C(17)	115.2 (3)	P(2)-C(12)-Si(2)	113.2 (4)
N-Si(1)-C(18)	112.1 (3)		

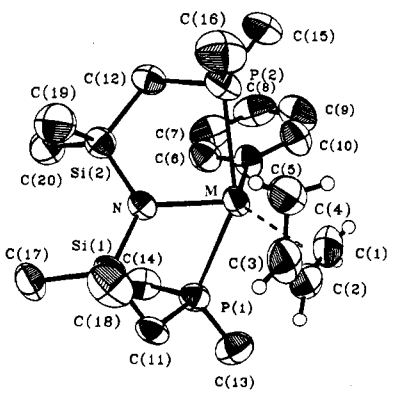

Figure 2. ORTEP plot of $M(\eta^4\text{-}C_4H_6)Ph[N(SiMe_2CH_2PMe_2)_2]$ [**3a** (M = Zr) and **3b** (M = Hf)] showing atom numbering scheme. Ellipsoids of non-hydrogen atoms are drawn at the 50% probability level.

derivative with comparisons made to the hafnium structure where appropriate (see Tables III–V).

Table V. Intraannular Torsion Angles (deg) with Standard Deviations in Parentheses

$Zr(C_4H_6)Ph[N(SiMe_2CH_2PMe_2)_2]$ (**3a**)	
N-Zr-P(1)-C(11)	-47.4 (3)
Zr-P(1)-C(11)-Si(1)	41.8 (3)
N-Si(1)-C(11)-P(1)	-14.2 (4)
C(11)-Si(1)-N-Zr	-33.9 (4)
P(1)-Zr-N-Si(1)	47.0 (3)
N-Zr-P(2)-C(12)	-33.0 (3)
Zr-P(2)-C(12)-Si(2)	40.8 (4)
N-Si(2)-C(12)-P(2)	-32.5 (5)
C(12)-Si(2)-N-Zr	-0.1 (4)
P(2)-Zr-N-Si(2)	19.3 (3)
C(4)-Zr-C(1)-C(2)	57.5 (8)
Zr-C(1)-C(2)-C(3)	-50.4 (11)
C(1)-C(2)-C(3)-C(4)	-4 (2)
C(2)-C(3)-C(4)-Zr	56.2 (10)
C(1)-Zr-C(4)-C(3)	-58.4 (8)
$Hf(C_4H_6)Ph[N(SiMe_2CH_2PMe_2)_2]$ (**3b**)	
N-Hf-P(1)-C(11)	-47.0 (3)
Hf-P(1)-C(11)-Si(1)	41.2 (3)
N-Si(1)-C(11)-P(1)	-14.4 (4)
C(11)-Si(1)-N-Hf	-32.8 (4)
P(1)-Hf-N-Si(1)	46.0 (2)
N-Hf-P(2)-C(12)	-31.5 (3)
Hf-P(2)-C(12)-Si(2)	38.8 (4)
N-Si(2)-C(12)-P(2)	-30.4 (5)
C(12)-Si(2)-N-Hf	-0.7 (4)
P(2)-Hf-N-Si(2)	19.0 (2)
C(4)-Hf-C(1)-C(2)	59.6 (5)
Hf-C(1)-C(2)-C(3)	-52.8 (8)
C(1)-C(2)-C(3)-C(4)	-1.4 (12)
C(2)-C(3)-C(4)-Hf	55.7 (7)
C(1)-Hf-C(4)-C(3)	-59.9 (5)

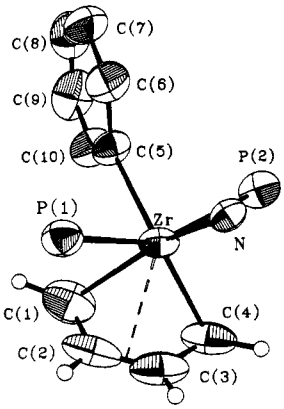

Figure 3. View of $Zr(\eta^4\text{-}C_4H_6)Ph[N(SiMe_2CH_2PMe_2)_2]$ (**3a**), showing the distorted octahedral environment around the metal center. The ligand backbone and the substituents at phosphorus have been removed for clarity. The octahedral coordination is obtained by ignoring the dotted line for the π-interaction.

The geometry about zirconium can be described as distorted octahedral if the C_4H_6 fragment is assigned two coordination sites (Figure 3). The tridentate amido–diphosphine ligand adopts an approximate meridional mode of coordination as indicated by the P1–Zr–P2 angle of 149° and an essentially planar set of donor atoms (N, P1, P2) and metal center. As has been discussed previously, an ideal meridional geometry having a P–M–P angle of 180° is impossible for this ligand system coordinated to the early metals because of the combination of long M–P bond lengths (Zr–P1, 2.752 (2) Å; Zr–P2, 2.730 (2) Å) and the short M–N bond (Zr–N, 2.190 (6) Å). The $Zr\text{–}C_{ipso}$ bond length of the phenyl group is 2.317 (7) Å ($Hf\text{–}C_{ipso}$, 2.290 (6) Å); this bond lies in a plane containing the Zr–N and the Zr–B (B is the center of gravity of the C_4H_6 unit) bonds such that the sum of the angles defined by N–Zr–C5, N–Zr–B, and C5–Zr–B is 358.8° (for the hafnium complex,

the sum is 358.9°). The butadiene unit is bonded to the zirconium with the following bond distances: Zr–Cl, 2.410 (12) Å; Zr–C2, 2.481 (11) Å; Zr–C3, 2.450 (9) Å; Zr–C4, 2.350 (10) Å; it is interesting to note that the average difference in distance from the inner and outer carbons to the metal center is only 0.09 Å. The C–C bond lengths are as follows: C1–C2, 1.40 (2) Å; C2–C3, 1.354 (15) Å; C3–C4, 1.442 (15) Å.

Comparisons of the distances and angles in the two structures discussed here and other related structures are revealing. Two different methods utilizing solid-state crystallographic data have been published to compare diene metal interactions, in particular, to gauge the component of π,η^4 verses σ^2,π to the bonding. The first method[26] compares the bond lengths M–C2 (or M–C3), C1–C2 (or C3–C4) and the bond angles M–C1–C2 (or M–C3–C4) as a group between different molecules. The higher this group of values is, the more the σ^2,π-form contributes to the bonding. For example, the complex $(\eta^5\text{-}C_5H_5)_2Zr$(diene) (diene = η^4-2,3-bis(methylene)bicyclo[2,2,1]heptane), having the values 2.550 (5) Å, 1.445 (2) Å, and 81.8 (1)°, shows the greatest degree of π,η^4-bonding for the series of zirconocene diene complexes, while the complex $(\eta^5\text{-}C_5H_5)_2Zr$(indanediyl), having the values 2.885 (4) Å, 1.48 (1) Å, and 95.8°, is considered to be purely σ^2 since the π-component is essentially nonbonding because it is part of the aromatic ring. The zirconium butadiene complex **3a** has the corresponding values of 2.466 (11) Å, 1.42 (2) Å, and 76.3 (7)°, which indicates more π,η^4-character than any of the isolated zirconocene diene complexes. The analogous hafnium butadiene complex **3b** has the values 2.456 (7) Å, 1.429 (12) Å, and 76.5 (5)°, very nearly identical with the zirconium derivative and also indicative of a substantial π,η^4-component to the bonding description. In addition, a relevant comparison is the formally hafnium(0) complex[27] $Hf(C_4H_6)_2$(dmpe) (dmpe = 1,2-bis(dimethylphosphino)ethane) which has the corresponding values 2.400 (5) Å, 1.437 (8) Å, and 74°; these low values suggest that increased π,η^4-character is enhanced by phosphorus donors.

The second method of comparison for diene complexes is more general and has been applied across the periodic table.[28] It has been found that an empirical relationship exist between the dihedral angle ϕ (defined as the angle subtended by the plane of the diene carbons and the plane containing the M, Cl, and C4 atoms) and Δd, where $\Delta d = \{d(\text{M–C1}) + d(\text{M–C}_4)\}/2 - \{d(\text{M–C2}) + d(\text{M–C3})\}/2$; this Δd parameter is the difference in distance of the metal from the inner carbons and the outer carbons. Both of these parameters are sensitive to the type of bonding in the complex. Late-transition-metal dienes derivatives all have ϕ in the range 75–90° and Δd varying between –0.1 and +0.1 Å and are diagnostic of the π,η^4-character of the bonding. On the other hand, early metal diene complexes generally have ϕ greater than 90° and Δd varies from –0.5 to 0 Å. For zirconocene and hafnocene diene complexes $(\eta^5\text{-}C_5H_5)_2M$(diene), ϕ is >110° and Δd is in the range –0.5 to –0.3 Å. Our zirconium butadiene complex **3a** has ϕ = 98.9° and Δd = –0.171 Å, and the hafnium derivative **3b** has ϕ = 97.5° and Δd = –0.193 Å, again indicating more π,η^4-character to the bonding than the aforementioned group 4 metallocene derivatives. Indeed, these values of

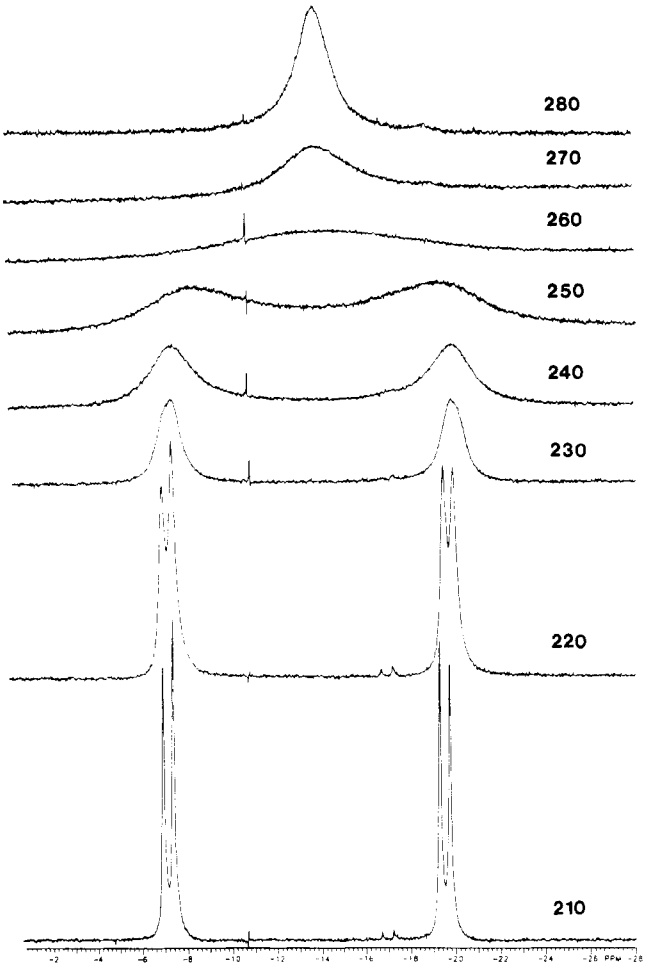

Figure 4. Variable-temperature $^{31}P\{^1H\}$ NMR spectra (C_7D_8) for $Hf(\eta^4\text{-}C_4H_6)Ph[N(SiMe_2CH_2PMe_2)_2]$ (**3b**).

ϕ and Δd for **3a** and **3b** place them in a region beyond any other group 4 diene complexes with the exception of $Hf(C_4H_6)_2$(dmpe).[27]

Previous comparisons between pairs of diene complexes that are different only by virtue of the central metal (i.e., Zr vs Hf) are consistent with the Hf derivatives having more σ-character to the bonding than the Zr analogues. This is evident from the shorter M–C2 (or M–C3) (metal-to-inner carbons) distances found for the zirconium complexes inspite of the fact that Hf–C bond lengths are generally shorter than the corresponding Zr–C bonds.[29] In the pair of complexes **3a** and **3b**, shorter Hf–C bond lengths are observed from the metal to C_{ipso} of the phenyl and from the metal to the terminal carbons of the butadiene unit as expected; however, the metal-to-inner carbon bond distances, M–C2 and M–C3, are virtually identical irrespective of the metal. This suggests that the relative amounts of σ^2,π vs π,η^4 bond character are independent of the metal in these systems, rather, it is the ancillary ligand that dominates.

Solution Structures and Dynamics. All of the new, group 4 butadiene complexes reported here display remarkably similar solution behavior, only mildly dependent (see Tables VI and VII) on the central metal (Zr vs Hf), the substituents at phosphorus (methyl vs isopropyl) and the other ligands (chloride vs hydrocarbyl). For this reason the solution spectroscopic data of only the hafnium phenyl complex **3b** will be discussed in detail.

(26) (a) Erker, G.; Engel, K.; Kruger, C.; Muller, G. *Organometallics* **1984**, *3*, 128–133. (b) Kruger, C.; Muller, G.; Erker, G.; Dorf, U.; Engel, K. *Organometallics* **1985**, *4*, 215–223. (c) See also ref 1a.

(27) Wreford, S. S.; Whitney, J. F. *Inorg. Chem.* **1981**, *20*, 3918–3924.

(28) Yasuda, H.; Nakamura, A.; Kai, Y.; Kasai, N. *Topics in Physical Organometallic Chemistry*; Freund Publishing House: 1987; Vol. 2, See also ref 1c and 5b.

(29) Hunter, W. E.; Atwood, J. A. *J. Organomet. Chem.* **1981**, *204*, 67–74.

Table VI. ^{1}H NMR Data (in ppm)[c]

compound	$SiMe_2$	PCH_2Si	PMe_2	P-$(CHMe_2)_2$	P-$(CHMe_2)_2$	C_4H_6	other
$Zr(C_4H_6)Cl[N(SiMe_2CH_2PMe_2)_2]$ (**2a**)[a]	0.14 (s) 0.22 (s)	0.65 (m)	0.94 (t) J_{app} = 3.5 1.20 (t) J_{app} = 3.5			H_a, 0.78 (m) H_s, 2.57 (m) H_m, 5.85 (m)	
$Hf(C_4H_6)Cl[N(SiMe_2CH_2PMe_2)_2]$ (**2b**)[a]	0.20 (s) 0.26 (s)	0.64 (dt) J_{gem} = 12 J_{app} = 5 0.70 (dt) J_{app} = 5	0.97 (t) J_{app} = 3.5 1.21 (t) J_{app} = 3.5			H_a, 0.63 (m) H_s, 2.03 (m) H_m, 6.04 (m)	
$Zr(C_4H_6)Cl[N(SiMe_2CH_2P(CHMe_2)_2)_2]$ (**2c**)[b]	0.25 (s) 0.30 (s)	0.75 (dt) J_{gem} = 14 J_{app} = 3.5 0.94 (dt) J_{app} = 4.5		1.95 (m) 2.30 (m)	1.06 (m) 1.09 (m) 1.11 (m) 1.25 (dt) $^3J_{H-H}$ = 7 J_{app} = 7	H_a, 1.15 (m) H_s, 2.53 (m) H_m, 6.02 (m)	
$Hf(C_4H_6)Cl[N(SiMe_2CH_2P(CHMe_2)_2)_2]$ (**2d**)[a]	0.40 (s) 0.44 (s)	0.81 (dt) J_{gem} = 14 J_{app} = 3.5 0.97 (dt) J_{app} = 3.5		2.05 (m) 2.34 (m)	1.17 (m) 1.18 (m) 1.20 (m) 1.30 (dt) $^3J_{H-H}$ = 7 J_{app} = 7	H_a, 1.00 (m) H_s, 2.19 (m) H_m, 6.37 (m)	
$Zr(C_4H_6)Ph[N(SiMe_2CH_2PMe_2)_2]$ (**3a**)[a]	0.13 (s) 0.24 (s)	0.61 (m)	0.75 (t) J_{app} = 3.0 0.88 (t) J_{app} = 3.0			H_a, 0.46 (m) H_s, 2.64 (m) H_m, 5.86 (m)	$Zr(C_6H_5)$ H_p, 7.14 (t) J_{app} = 7.0 H_m, 7.28 (t) J_{app} = 7.0 H_o, 7.76 (d) J_{app} = 7.0
$Hf(C_4H_6)Ph[N(SiMe_2CH_2PMe_2)_2]$ (**3b**)[a]	0.20 (s) 0.30 (s)	0.70 (t) J_{app} = 4.5	0.79 (t) J_{app} = 3.0 0.97 (t) J_{app} = 3.0			H_a, 0.53 (m) H_s, 2.24 (m) H_m, 6.02 (m)	$Hf(C_6H_5)$ H_p, 7.15 (t) J_{app} = 7.0 H_m, 7.32 (t) J_{app} = 7.0 H_o, 7.81 (d) J_{app} = 7.0
$Zr(C_4H_6)CH_2CMe_3[N(SiMe_2CH_2PMe_2)_2]$ (**4a**)[a]	0.18 (s) 0.30 (s)	0.66 (m)	0.94 (t) J_{app} = 3.0 1.11 (obscured)			H_a, 0.32 (m) H_s, 2.21 (m) H_m, 6.06 (m)	$Zr(CH_2CMe_3)$ H_α, obscured H_γ, 1.10 (s)
$Hf(C_4H_6)CH_2CMe_3[N(SiMe_2CH_2PMe_2)_2]$ (**4b**)[a]	0.22 (s) 0.30 (s)	0.58 (dt) J_{app} = 4.0 J_{gem} = 14 0.74 (dt) J_{app} = 4.0	0.96 (t) J_{app} = 2.8 1.12 (t) J_{app} = 2.8			H_a, 0.20 (m) H_s, 1.78 (m) H_m, 6.17 (m)	$Hf(CH_2CMe_3)$ H_α, 0.05 (t) J_{app} = 4.5 H_γ, 1.10 (s)

[a] In C_6D_6. [b] In C_7H_8. [c] Coupling constants in hertz.

Inspection of the temperature dependent $^{31}P\{^1H\}$ NMR spectrum of **3b**, shown in Figure 4, and comparison to the structure as determined in the solid-state (Figure 2) necessitates that some fluxional process be invoked. The solid-state structure has no symmetry and would require that there be two inequivalent phosphorus nuclei; however, the singlet observed in the high-temperature limit requires some process that exchanges the two ends of the meridionally bound ancillary ligand. The room-temperature ^{1}H NMR spectrum of **3b** is shown in Figure 5a. Besides the typical pattern for the phenyl group downfield, the resonances associated with the ancillary amido–diphosphine ligand consist of two singlets for the silylmethyls, two pseudotriplets for the phosphorus methyls, and two degenerate pseudotriplets for the methylene protons (PCH_2Si). The butadiene unit shows only three multiplets (worth two hydrogens each) at 6.02, 2.24, and 0.53 ppm assigned to the hydrogens at C2 and C3 (H_{meso}), the outer hydrogens at C1 and C4 (H_{syn}), and the inner hydrogens at C1 and C4 (H_{anti}), respectively. Finally and most importantly, the ambient-temperature $^{13}C\{^1H\}$ NMR spectrum of **3b** shows only two carbon resonances for the butadiene fragment. All of these spectra change as a function of temperature to give limiting spectra which are consistent with the solid-state structure. The singlet in the $^{31}P\{^1H\}$ NMR spectrum becomes an AX pattern at low temperature (Figure 4) indicating two inequivalent phosphines coupled to each other; the low-temperature limiting ^{1}H NMR spectrum (Figure 5b) shows four silylmethyl resonances, four phosphorus methyl peaks, and resonances consist with six inequivalent protons on the butadiene moiety (the inequivalent anti protons, H_{anti}, are obscured). Also the low-temperature $^{13}C\{^1H\}$ NMR spectrum shows four different carbon resonances for the butadiene fragment (see Table VIII).

This dynamic behavior cannot be adequately explained by using the envelope flip mechanism that is typical for early metal diene complexes (see Scheme I). For example, if the diene were flipping, then the high-temperature-limiting ^{1}H NMR spectrum of the butadiene moiety should show two types of H_{meso} (worth one proton each) and two resonances for the average of H_{syn} and H_{anti} on the inequivalent terminal carbons. In addition, the diene flipping mechanism cannot account for only two types of carbons in the fast-exchange limit; were this mechanism operative, all four carbons would remain inequivalent at all temperatures. The only data that are consistent with the diene flipping process are the phosphorus NMR spectra.

The simplest process that accounts for all of the variable-temperature solution spectroscopic data is diene rotation (Scheme II). In the fast-exchange limit, diene

Table VII. ^{13}C NMR Data (in ppm)[c]

compound	$SiMe_2$	PCH_2Si	PMe_2	P-$(CHMe_2)_2$	P-$(CHMe_2)_2$	C_4H_6[d]	other
$Zr(C_4H_6)Cl[N(SiMe_2CH_2PMe_2)_2]$ (**2a**)[a]	5.36 (s) 5.85 (s)	17.99 (m)	13.62 (t) J_{app} = 6.9			C_t, 60.21 (s) C_i, 89.63 (s)	
$Hf(C_4H_6)Cl[N(SiMe_2CH_2PMe_2)_2]$ (**2b**)[b]	5.55 (s) 6.18 (s)	17.64 (s)	13.48 (t) J_{app} = 6.8 13.87 (t) J_{app} = 8.5			C_t, 56.87 (s) [t, 141.9] C_i, 114.76 (s) [d, 156.5]	
$Zr(C_4H_6)Cl[N(SiMe_2CH_2P(CHMe_2)_2)_2]$ (**2c**)[b]	5.71 (s) 6.46 (s)	10.47 (t) J_{app} = 2.7		25.04 (t) J_{app} = 4.8 25.24 (t) J_{app} = 3.7	18.72 (s) 19.09 (s) 19.42 (s) 19.60 (s)	C_t, 61.64 (s) [t, 146.0] C_i, 113.06 (s) [d, 157.7]	
$Hf(C_4H_6)Cl[N(SiMe_2CH_2P(CHMe_2)_2)_2]$ (**2d**)[b]	5.77 (s) 6.40 (s)	9.72 (br)		24.73 (t) J_{app} = 4.2 25.11 (t) J_{app} = 5.1	18.62 (s) 19.16 (s) 19.45 (s) 19.57 (s)	C_t, 57.91 (s) [t, 145] C_i, 114.62 (s) [d, 164.1]	
$Zr(C_4H_6)Ph[N(SiMe_2CH_2PMe_2)_2]$ (**3a**)[a]	5.91 (br)	17.87 (s)	13.99 (t) J_{app} = 6.6 14.45 (t) J_{app} = 5.6			C_t, 59.8 (s) C_i, 115.0 (s)	$Zr(C_6H_5)$ C_p, 124.7 (s) C_m, 126.4 (s) C_o, 135.6 (t) J_{app} = 3 C_i, 191.8 (t) J_{app} = 6
$Hf(C_4H_6)Ph[N(SiMe_2CH_2PMe_2)_2]$ (**3b**)[b]	5.79 (s) 6.20 (s)	17.74 (s)	14.02 (t) J_{app} = 7.8 14.41 (t) J_{app} = 6.1			C_t, 57.0 (s) [t, 145.2] C_i, 112.1 (s) [d, 154]	$Hf(C_6H_5)$ C_p, 124.4 (s) C_m, 126.9 (s) C_o, 137.2 (t) J_{app} = 3 C_i, 197.9 (t) J_{app} = 3
$Zr(C_4H_6)CH_2CMe_3[N(SiMe_2CH_2PMe_2)_2]$ (**4a**)[a]	5.91 (s) 5.95 (s)	17.95 (s)	13.8 (t) J_{app} = 5.1 14.26 (t) J_{app} = 5.1			C_t, 56.30 (s) C_i, 109.54 (s)	$Zr(CH_2CMe_3)$ C_α, 82.51 (s) C_β, 36.35 (s) C_γ, 35.41 (s)
$Hf(C_4H_6)CH_2CMe_3[N(SiMe_2CH_2PMe_2)_2]$ (**4b**)[a]	5.85 (s) 6.05 (s)	17.76 (s)	13.52 (t) J_{app} = 6.3 14.22 (t) J_{app} = 6.1			C_t, 54.93 (s) [t, 143.0] C_i, 110.7 (s) [d, 157.0]	$Hf(CH_2CMe_3)$ C_α, 83.06 (s) [t, 101.0] C_β, 36.35 (s) C_γ, 35.07 (s) [t, 124.0]

[a] In C_6D_6. [b] In C_7D_8. [c] Coupling constants in hertz. [d] $^1J_{C-H}$ in square brackets.

Table VIII. Low-Temperature Diene ^{13}C NMR Data (in C_7D_8 in ppm)

compd	temp, K	carbons: inner	carbons: outer
$Zr(C_4H_6)Cl[N(SiMe_2CH_2PMe_2)_2]$ (**2a**)	193	120, 108	not resolved
$Hf(C_4H_6)Cl[N(SiMe_2CH_2PMe_2)_2]$ (**2b**)	190	118.2, 110.1	56.1, 55.8
$Zr(C_4H_6)Cl[N(SiMe_2CH_2P(CHMe_2)_2)_2]$ (**2c**)	180	116, 110	62, 58
$Hf(C_4H_6)Cl[N(SiMe_2CH_2P(CHMe_2)_2)_2]$ (**2d**)	180	not resolved	not resolved
$Zr(C_4H_6)Ph[N(SiMe_2CH_2PMe_2)_2]$ (**3a**)	188	120.6, 101.2	63.2, 55.1
$Hf(C_4H_6)Ph[N(SiMe_2CH_2PMe_2)_2]$ (**3b**)	190	120.9, 103.9	57.8, 54.4
$Hf(C_4H_6)CH_2CM)_3[N(SiMe_2CH_2PMe_2)_2]$ (**4b**)	190	110.3, 108.2	55.7, 52.5

rotation equilibrates the two phosphorus donors of the ligand, the meso, anti and syn pairs of protons on the butadiene fragment, and the two carbon pairs. The room-temperature ^1H NMR spectrum is now interpretable if one assumed that the solid-state structure is maintained in solution with only the diene rotating on the NMR time scale. Because of the presence of the phenyl group on one side of the meridional plane of the amido–diphosphine, the ligand displays resonances associated with different environments above and below this meridional plane. This is confirmed by nOe difference spectroscopy which only shows an enhancement of the *o*-phenyl protons when the *downfield* silylmethyl group is irradiated.

Scheme I

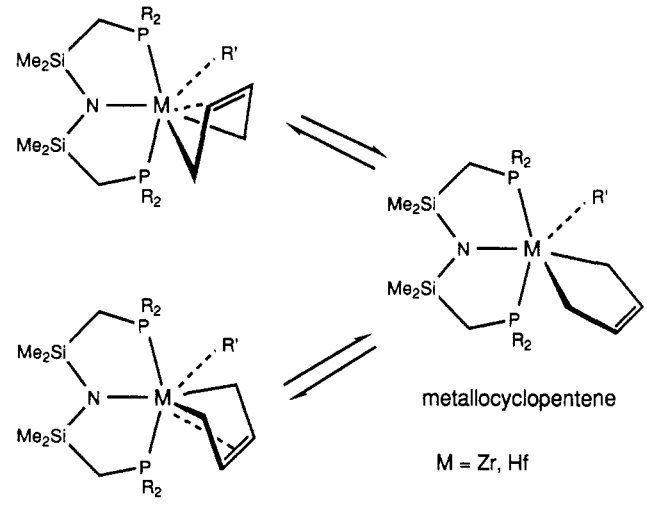

The activation free energies, $\Delta G^\ddagger$, for the diene rotation process can be determined easily from the variable-temperature $^{31}P\{^1H\}$ NMR spectral data by standard techniques (see Experimental Section) and are lised in Table IX with the phosphorus-31 chemical shift and coupling constant data. As a group, $\Delta G^\ddagger$ ranges only from 9.1 to 12.3 kcal mol^{-1}, and for each pair having different central metals, the hafnium complexes have lower barriers but only by 0.5–0.9 kcal mol^{-1}. This is in contrast to the metallocene complexes (η^5-$C_5H_5)_2Zr(C_4H_6)$ and (η^5-

Table IX. ^{31}P NMR Data (in C_7D_8)

	temp, K	$\Delta G^{\ddagger}$, kcal mol^{-1}	chem shift, ppm	$^2J_{P-P}$, Hz
$Zr(C_4H_6)Cl[N(SiMe_2CH_2PMe_2)_2]$ (**2a**)	270		−18.02	
	180	11.3	−15.08, −20.99	76.1
$Hf(C_4H_6)Cl[N(SiMe_2CH_2PMe_2)_2]$ (**2b**)	293		−10.29	
	184	10.7	−9.89, −19.70	79.8
$Zr(C_4H_6)Cl[N(SiMe_2CH_2P(CHMe_2)_2)_2]$ (**2c**)	293		+16.53	
	180	9.6	+19.00, +11.65	78.9
$Hf(C_4H_6)Cl[N(SiMe_2CH_2P(CHMe_2)_2)_2]$ (**2d**)	293		+26.83	
	180	9.1	+30.07, +13.03	76.9
$Zr(C_4H_6)Ph[N(SiMe_2CH_2PMe_2)_2]$ (**3a**)	288		−18.76	
	180	11.5	−17.21, −19.16	62.3
$Hf(C_4H_6)Ph[N(SiMe_2CH_2PMe_2)_2]$ (**3b**)	280		−13.78	
	180	10.9	−7.33, −18.95	53.2
$Zr(C_4H_6)CH_2CMe_3[N(SiMe_2CH_2PMe_2)_2]$ (**4a**)	296		−17.46	
	180	12.3	−13.25, −19.36	78.8
$Hf(C_4H_6)CH_2CMe_3[N(SiMe_2CH_2PMe_2)_2]$ (**4b**)	303		−11.95	
	190	11.4	+4.74, −15.36	77.0

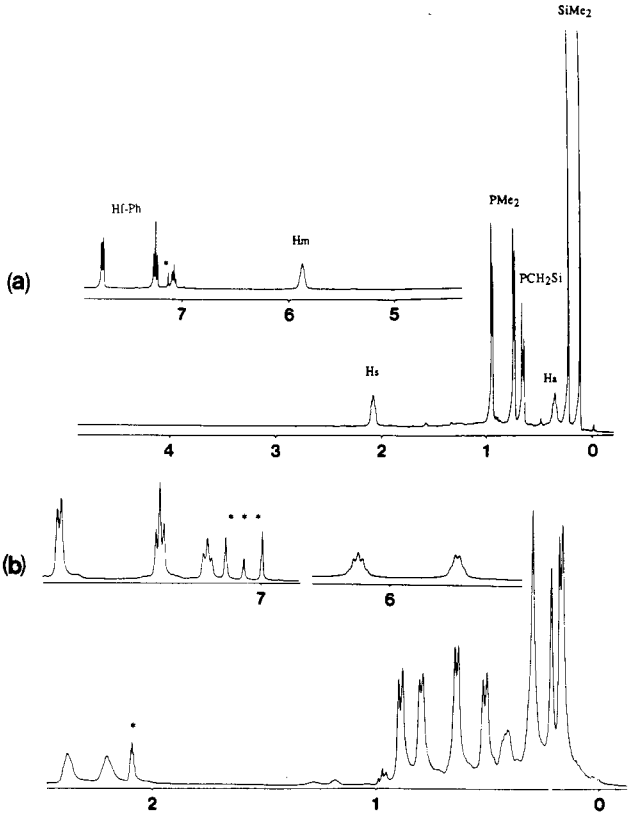

Figure 5. ^1H NMR spectra of $Hf(\eta^4\text{-}C_4H_6)Ph[N(SiMe_2CH_2PMe_2)_2]$ (**3b**): top spectrum, (a) room temperature in C_6D_6; bottom spectrum, (b) −80 °C in C_7D_8. The asterisks in both spectra indicate residual solvent peaks.

$C_5H_5)_2Hf(C_4H_6)$ that show barriers to diene flipping of 12.6 and 8.1 kcal mol^{-1}, respectively. The large difference between Zr and Hf in the metallocenes has been ascribed to a higher component of σ^2,π-character to the bonding for Hf over Zr. As has already been pointed out in the discussion of the solid-state structures of **3a** and **3b**, there is little dependence on the central metal in the metrical parameters of the molecular structures and the activation barriers mirror that in solution as well.

Although the variation in $\Delta G^{\ddagger}$ is not large, it is interesting to note that the two complexes with the lowest barriers are the derivatives with isopropyl substituents at phosphorus, **2c** and **2d**. Rather than slow the fluxional process down, the presence of bulky substituents at phosphorus appears to accelerate the diene movement. This is reasonable if one assumes that even in the modified meridional coordination mode displayed by this amido-diphosphine ligand, there is a slight bond weakening of the

Scheme II

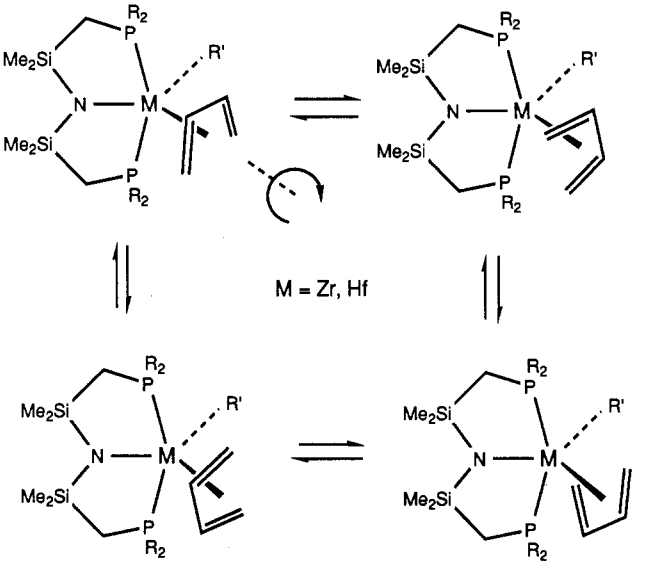

butadiene fragment because of steric repulsion. This accelerated diene movement is also in accord with the accelerated carbon–carbon coupling observed[14] for the complexes with the bulky isopropyl substituents.

One final point concerns the possibility of fluxional processes other than diene flipping or diene rotation. Processes can be invoked that involve one phosphine arm of the ancillary ligand dissociating to generate a five-coordinate intermediate which rapidly rearranges via a Berry pseudorotation or a turnstile mechanism.[30] Such a sequence is difficult to reconcile with the data, however. In particular, were such massive structural rearrangements operative, then the $\Delta G^{\ddagger}$ values would be very sensitive to the substituents at phosphorus and the other ligands at the metal, but no such variation is observed. The possibility of a *mer* to *fac* isomerization of the ancillary ligand without phosphine dissociation can also be excluded because of the lack of variation in $\Delta G^{\ddagger}$ and also because of the nOe difference spectroscopic results that require the phenyl ligand to be on the same side of the ligand even in the fast-exchange limit.

Conclusions

The incorporation of phosphine donors to stabilize 1,3-butadiene complexes of the group 4 metals Zr and Hf has noteworthy consequences. The X-ray crystallographic data are consistent with the 1,3-butadiene unit having sub-

(30) Berry, R. S. *J. Chem. Phys.* **1960**, *32*, 933–938.

stantial π,η^4-character, more so than is present in the $(\eta^5\text{-}C_5H_5)_2M(\text{diene})$ (M = Zr, Hf) complexes. This in turn suggests that the M(II) oxidation state contributes significantly to the bonding scheme of the derivatives $M(\eta^4\text{-}C_4H_6)R'[N(SiMe_2CH_2PR_2)_2]$.

These new group 4 butadiene complexes display fluxional behavior that is best described as diene rotation rather than the envelope-flipping mechanism normally associated with early metal diene derivatives. That this fluxional process is more akin to that found for an electron-rich, late-transition-metal complex provides further support for the proposal that phosphine donors can stabilize lower oxidation states of the early transition metals.[31]

(31) For recent examples of this strategy, see: (a) Wielstra, Y.; Gambarotta, S.; Roedelof, J. B.; Chiang, M. Y. *Organometallics* **1988**, *7*, 2177. (b) Wielstra, Y.; Gambarotta, S.; Chiang, M. Y. *Organometallics* **1988**, *7*, 1866.

Acknowledgment. Financial support was provided by NSERC of Canada. Acknowledgment is also made to the donors of the Petroleum Research Fund, administered by the American Chemical Society, for the partial support of this work. We are also grateful to Professor James Trotter for the use of his diffractometer and structure solving programs.

Registry No. **1a**, 94372-15-3; **1b**, 98758-74-8; **1c**, 94372-17-5; **1d**, 94372-16-4; **2a**, 120638-28-0; **2b**, 113686-58-1; **2c**, 120638-29-1; **2d**, 113686-59-2; **3a**, 120638-30-4; **3b**, 120638-31-5; **4a**, 120638-32-6; **4b**, 120665-67-0; $Mg\text{-}C_4H_6$, 60300-64-3; LiPh, 591-51-5; $LiCH_2CMe_3$, 7412-67-1.

Supplementary Material Available: Tables of calculated hydrogen atom parameters, anisotropic thermal parameters, and bond lengths and angles involving refined hydrogen atoms (Tables S1–S4) (5 pages); listings of structure factors (Tables S5 and S6) (50 pages). Ordering information is given on any current masthead page.

A Survey of Catalytic Activity of η^5-Cyclopentadienyl Complexes of Groups 4–6 and Uranium and Thorium for the Dehydrocoupling of Phenylsilane

Clare Aitken, Jean-Pierre Barry, Francois Gauvin, John F. Harrod,* Abdul Malek, and Denis Rousseau

Department of Chemistry, McGill University, Montreal, PQ, Canada, H3A 2K6

Received December 2, 1988

The effectiveness of a variety of metallocene, metallocene alkyl, and metallocene hydride complexes of group 4–6 metals and of U and Th as catalysts for the dehydrocoupling of phenylsilane was studied. Among the d-block complexes only those of Ti and Zr showed high activity for the production of higher oligomers (degree of polymerization 10–20). Vanadocene is an effective catalyst for the synthesis of 1,2-diphenyldisilane and 1,2,3-triphenyltrisilane from phenylsilane but under much more forcing condition than necessary with the group 4 catalysts. The metallocene hydrides of Mo, W, Nb, and Ta react slowly with phenylsilane to give relatively stable metallocene silyl hydrides or other decomposition products that show no catalytic activity. The synthesis and characterization of a number of new hydridosilylmolybdenocene complexes are described. Although the organouranium and -thorium complexes show some catalytic activity for dehydrocoupling of phenylsilane in ether solution, their instability and the complexity of the chemistry involved mitigates against their usefulness as practical catalysts. An explanation of the unique activity of Ti and Zr complexes is proposed that invokes the necessity for an empty nonbonding orbital on the metal to facilitate an α-hydrogen elimination from coordinated silyl ligand.

Introduction

A number of promising applications of polysilanes has recently aroused considerable interest in their synthesis and the study of their physical and chemical properties.[1] The only known route to poly(organosilanes) of high molecular weight is the condensation of diorganodihalosilanes through reaction with a group 1 metal (the Wurtz–Fittig reaction).[2,3] Although this method is highly versatile and can give linear polymers with molecular weights up to ca. 10^6, it suffers from the fact that it is difficult to control and usually gives large amounts of cyclic oligomers and/or a low molecular weight fraction.

The discovery of catalysts for the facile dehydrocoupling of primary organosilanes aroused hopes that such reactions might provide another, and perhaps superior, synthesis of polysilanes.[4–6] The first class of catalysts explored by us were compounds of the type Cp_2MR_2, where Cp is an

(1) West, R.; Maxka, J. In *Inorganic and Organometallic Polymers*; Zeldin, M.; Wynne, K. J.; Allcock, H. R., Eds.; ACS Symposium Series 360; American Chemical Society: Washington, DC, 1988; Chapter 2 and references therein.

(2) Burkhard, C. A. *J. Am. Chem. Soc.* **1949**, *71*, 963. Kumada, M.; Tamao, K. *Adv. Organomet. Chem.* **1968**, *6*, 19. West, R. *Pure Appl. Chem.* **1982**, *54*, 1041. Hengge, E. *Top. Curr. Chem.* **1974**, *51*, 1. Yajima, S.; Hayashi, J.; Omori, M. *Chem. Lett.* **1975**, 931.

(3) West, R.; David, L. D.; Djurovic, P. I.; Stearley, K. L.; Srinivasan, K. S. V.; Yu, H. *J. Am. Chem. Soc.* **1981**, *103*, 7352. Trujillo, R. E. *J. Organomet. Chem.* **1980**, *198*, C27. Wesson, J. P.; Williams, T. C. *J. Polym. Sci., Polym. Chem. Ed.* **1979**, *17*, 2833.

(4) (a) Aitken, C. T.; Harrod, J. F.; Samuel, E. *J. Organomet. Chem.* **1985**, *279*, C11. (b) Aitken, C. T.; Harrod, J. F.; Samuel, E. *J. Am. Chem. Soc.* **1986**, *108*, 4059. (c) Aitken, C. T.; Samuel, E.; Harrod, J. F. *Can. J. Chem.* **1986**, *64*, 1677. Harrod, J. F.; Yun, S. S. *Organometallics* **1987**, *6*, 1381.

(5) Harrod, J. F. *Inorganic and Organometallic Polymers*; Zeldin, M., Wynne, K. J., Allcock, H. R., Eds.; ACS Symposium Series 360; American Chemical Society: Washington, DC, 1988; Chapter 7. Harrod, J. F. *The Design, Activation and Transformation of Organometallics into Common and Exotic Materials*; Laine, R. M., Ed.; NATO ASI Series E, 141; Martinus Nijhoff: Amsterdam, 1988; p 103.

(6) Aitken, C. T.; Harrod, J. F.; Gill, U. S. *Can. J. Chem.* **1987**, *65*, 1804.

0276-7333/89/2308-1732$01.50/0